IEEE Access
Multidisciplinary ⋮ Rapid Review ⋮ Open Access Journal

Received May 2, 2020, accepted May 15, 2020, date of publication June 9, 2020, date of current version June 23, 2020.

Digital Object Identifier 10.1109/ACCESS.2020.3001191

Cardiomyocytes: Analysis of Temperature Response and Signal Propagation Between Dissociated Clusters Using Novel Video-Based Movement Analysis Software

DHANESH KATTIPPARAMBIL RAJAN[1], (Member, IEEE), ANTTI-JUHANA MÄKI[1], MARI PEKKANEN-MATTILA[2], (Member, IEEE), JOOSE KREUTZER[1], TOMI RYYNÄNEN[1], HANNU VÄLIMÄKI[1], JARMO VERHO[1], JUSSI T. KOIVUMÄKI[2,3], HEIMO IHALAINEN[1], KATRIINA AALTO-SETÄLÄ[2,3,4,5], PASI KALLIO[1], AND JUKKA LEKKALA[1]

[1]Micro- and Nanosystems Research Group, Faculty of Medicine and Health Technology, Tampere University, 33720 Tampere, Finland
[2]Heart Group, Faculty of Medicine and Health Technology, Tampere University, 33520 Tampere, Finland
[3]Computational Biophysics and Imaging Group, Faculty of Medicine and Health Technology, Tampere University, 33520 Tampere, Finland
[4]Heart Hospital, Tampere University Hospital, 33520 Tampere, Finland
[5]Clinical Medicine, Faculty of Medicine and Health Science, Tampere University, 33520 Tampere, Finland

Corresponding author: Dhanesh Kattipparambil Rajan (dhanesh.kr@tuni.fi)

This work was supported by the Business Finland [former Finnish Funding Agency for Technology and Innovation (TEKES)] through the Human Spare Parts 2 Project.

ABSTRACT Human-induced pluripotent stem cell-derived cardiomyocytes (hiPSC-CMs) provide a great resource for functional cell and tissue models that can be applied in heart research, pharmaceutical industry, and future regenerative medicine. During cell model experiments, precise control of environmental parameters is important. Temperature is a fundamental parameter, and the acute effect of temperature on hiPSC-CM functions has previously been studied. This paper reports on long-term, systematic temperature response studies of hiPSC-CM cultures. The studies were conducted outside an incubator in a modular cell culturing system along with a temperature sensor plate (TSP) and a new beating analysis software (CMaN -cardiomyocyte function analysis tool). Temperature sensing at the actual cell location is challenging with bulky external sensors; however, a TSP with resistive microsensors provides an effortless solution. Experimental results showed that temperature nonlinearly affects the hiPSC-CM beating frequency with a Q_{10} temperature coefficient of ∼2.2. Both the active (contraction) and passive (relaxation) movements were influenced by temperature, and changes in the relaxation times were larger than the contraction times. However, the contraction amplitudes exhibited a greater spread of variation. We also present novel results on the visualization of hiPSC-CM contractile networking and non-invasive image-based measurement of signal propagation between dissociated CM clusters. Compared with previously reported tools, CMaN is an advanced and easy-to-use robust software. It is faster, more sensitive, computationally less expensive, and extracts six different signals of the contractile motion per process, providing at least one useful beating signal even in complex cases. The software also supports movement center detection and independent computation of the relaxation and contraction parameters.

INDEX TERMS Cardiomyocytes beating analysis software, movement center detection, cardiomyocytes temperature response, nonlinear temperature dependency, signal propagation between clusters.

I. INTRODUCTION

The limited availability of primary human cardiomyocytes (CMs) poses challenges for basic and translational research. However, human-induced pluripotent stem cells (hiPSC) can be differentiated into cardiomyocytes (hiPSC-CMs), providing an unlimited source of human CMs from healthy individuals and from patients with genetic cardiac diseases. hiPSC-CMs are a promising tool that can be used to study the development of the heart and CMs, cardiac disease

The associate editor coordinating the review of this manuscript and approving it for publication was Eduardo Rosa-Molinar.

modelling, and future regenerative medicine applications [1], [2]. Additionally, owing to their human origins, they overcome the limitations of animal models for drug screening and toxicology [3]. In hiPSC-CM experimental models, levels of O_2, CO_2, pH, and osmolarity are crucial to maintaining the functionalities of CMs. Temperature is another vital parameter, and it must be carefully regulated to maintain normal cardiac activity without hyper/hypothermia [4], [5]. In hibernation experiments, hypothermia has been shown to cause metabolic injuries and damage to mammalian hearts [6]. Additionally, functional and cellular injuries and field potential alterations have been reported in cultured CMs during hypothermia [7], [8]. Generally, both hypo- and hyperthermia induce stress in cells, which can generate various stress reactions [9]. Typical stress reactions involve the expression of cold or heat shock proteins, which can adversely affect vital cell functions [10]–[12]. Hypothermia/rewarming (H/R) cycles are known to reduce myofilament Ca^{2+} sensitivity and affect cardiac action potentials (AP) and contractility [13], [14]. They have also been shown to affect the sarcomere length and cardiac muscle force generation in animal models [14]–[16]. Generally, H/R is poorly tolerated by the myocardium, but a complete picture of the underlying mechanism of H/R-induced abnormalities is still elusive [14]. In the laboratory, cells often experience temperature shock when moved outside incubators or sometimes inside incubators. This can affect the cell attachment [17], pH [18], and evaporation rate, all of which can generate undesired stimulations and experimental variations [18]–[21]. In extreme cases, temperature shocks can trigger oxidative damage [10] and initiate cell death [22]. Therefore, it is important that the temperature-related stress responses of hiPSC-CMs are recognized and carefully evaluated.

The temperature responses can be studied in different ways, e.g., using standard electrophysiological methods, traction/atomic force microscopy, or video microscopy [23]. A decline in beating frequency has often been observed when CMs are collected from an incubator or studied at low temperatures [23]. However, precise temperature sensing from the cell area is typically challenging when using bulky external sensors [24], and the temperatures reported in many prior studies may correspond only approximately to the real temperatures experienced by CMs. This is because of difficulties in attaching temperature sensors closely to cells. Furthermore, to our knowledge, systematic, automated H/R temperature stressing and concurrent hiPSC-CM mechanobiological measurements have not been reported thus far. Few recent reports have described the excitation–contraction coupling during H/R and temperature-dependent beating synchronization [14], [25]. However, these studies were not conducted using hiPSC-CMs but with animal CMs. Herein, a long-term automated hiPSC-CM mechanobiological response to temperature was evaluated using a previously reported apparatus [26] and two new add-ons: 1) a temperature sensor plate (TSP) patterned with micro-temperature sensors and 2) novel video-based mechanobiology analysis software (CMaN - cardiomyocyte function analysis tool). By including the TSP, traditional bulky thermometers were avoided; instead, CMs were directly cultured on the TSP. This enabled accurate temperature sensing from the exact cell area. According to our experimental data analysis, the temperature dependence on hiPSC-CM beating frequency is nonlinear, which has not been previously reported. We also computed the Q_{10} temperature coefficients [27] of hiPSC-CMs. Moreover, we observed the contractile networking and beating synchronization of dissociated clusters and measured the propagation of the action potential (AP) signal between them. This is the first paper that reports these events in hiPSC-CM cultures and their non-invasive measurements by image processing.

The new software, CMaN, is an easy-to-use tool and available as Supplementary Material 1. Compared with conventional function analysis methods, such as Ca^{2+} transients, electrophysiology, sarcomere length profiling, or AFM approaches [25], [28]–[31], CMaN is a non-invasive and robust tool. The properties of several similar tools have been compared elsewhere [23], and CMaN was tested against three of them [32]–[34]. CMaN is faster, more sensitive, computationally less expensive, and allows ROI (region of interest) selection. It can process videos from single cells or large clusters individually or batchwise, and compared to previous methods [32]–[38], CMaN extracts six separate signals of the contractile motion per processing. The separate signals are especially advantageous when analyzing videos that have complex features, such as weak movements, overexposure, and gamma variations owing to uneven backgrounds. Additionally, the signals from CMaN represent the contractile phenomena more exactly with both positive (upstroke) and negative (downstroke) segments, allowing the computation of not only the beating frequency but also the contraction and relaxation features separately. Furthermore, optional features to detect the movement area (cluster location) and movement center (region of the largest contractile motion) were also integrated.

II. MATERIALS AND METHODS

A. DEVICE

The portable cell culture system [26] and in-house microfabricated temperature sensor plate [24] are shown in FIGURE 1. The temperature sensor plate contains independently calibrated resistive micro-temperature sensors that are patterned with copper on a glass plate, which senses temperature from the exact cell area (FIGURE 1c-e). The culture temperature is regulated with a programmable transparent indium tin oxide (ITO) heater [24]. Of the two microscopy options [26], inverted microscopy was utilized for recording the beating videos (camera: FL3-U3-13E4C-C, PointGrey-FLIR Systems). The culture was illuminated only during the video recordings. The hiPSC-CMs were cultured in a mini incubator (FIGURE 1b,c) made of a polydimethylsiloxane (PDMS) cell culture chamber [35] that was sealed with a

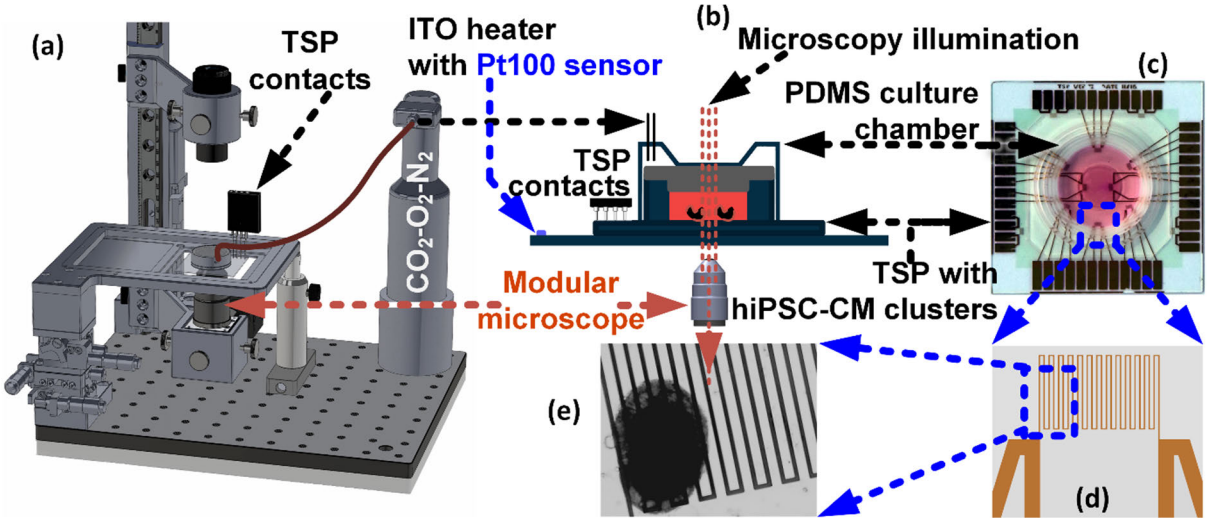

FIGURE 1. Apparatus for the hiPSC-CM temperature response experiments. (a) Portable modular cell culture system [26]. (b) Mini incubator. (c) Temperature sensor plate (TSP). The mini incubator is fixed on the TSP, and the ITO heater stays underneath. (d, e) A beating hiPSC-CM cluster on one of the resistive temperature sensors on the TSP. Beating signals were analyzed non-invasively from the recorded cell videos using CMaN software.

TABLE 1. CMaN performance comparison against MUSCLEMOTION and SarcTrack using two computers (System 1: 2.6-GHz processor and 32 GB of RAM, System 2: 2.7-GHz processor and 8 GB of RAM). †30-s long avi (60 fps, 640 × 512 pixels, 32-bit RGB, 1.64-GB size on an SSD hard drive). †2 20 avi files (33-GB size on an external SSD drive).

	MUSCLEMOTION	SarcTrack	CMaN	
Platform	Image J	MATLAB	MATLAB	
Algorithm principle	pixel intensity difference	fluorescent tag tracking	affine flow	
User ROI	no	no	yes	
Minimum ROI (pixels)	NA	NA	78 x 78	
Number of signals/processing	1	1	6	
Sensitivity	see FIGURE 4	NA	see FIGURE 4	
Processing time (~minutes)			**System1**	**System2**
1 video†	3 (6 in dynamic mode)	350	1	1.3
Batch†2 of videos	129	7390	25	28

transparent polycarbonate lid and polypropylene outer cover [39], [40]. A gas mixture (5 % CO_2, 19 % O_2, and 76 % N_2) supplied around the PDMS chamber created a stable gas environment [21]. The data flow and all the automated operations were controlled using a custom user interface that was scripted using MATLAB R2016B (MathWorks, Inc., Natick, MA, USA).

B. CELL CULTURING

The hiPSC-CMs were differentiated [41] by co-culturing iPS cells with END-2 cells [42] from the healthy control in-house iPS cell line (UTA.04602.WT). The beating hiPSC-CM clusters were mechanically excised from the differentiation cultures 20–30 days after initiation of differentiation and plated on the TSP. Before plating, TSPs were first sterilized with 70% ethanol and dried thoroughly before the mini incubator was attached to the plate. Plates were hydrophilized with fetal bovine serum (FBS, Lonza) and coated with 0.1% gelatin type A (Sigma-Aldrich). For each plate, 3–4 beating hiPSC-CM clusters were plated. After plating, the hiPSC-CM clusters were cultured in a conventional incubator overnight in KnockOut Dulbecco's Modified Eagle Medium (KO-DMEM, Lonza) with 20% FBS, 1% nonessential amino acids (NEAA, Cambrex), 2 mM Glutamax (Invitrogen), and 50 U/mL penicillin/streptomycin (Lonza) before transferring them onto the modular system. For all prolonged cell culturing, the exhausted culture medium was replaced with fresh medium twice a week.

C. ANALYSIS SOFTWARE

Herein, CMaN was scripted (in MATLAB), evaluated, and utilized. It is available as Supplementary Material 1 with this article. In CMaN, the movement analysis is based on a novel approach for the computation of the affine optic flow, which is an improved version of the classical Lucas–Kanade optical flow method that estimates the velocity of objects in consecutive images [43]. In the affine optic flow, the flow field is parameterized [44], [45] by a six-dimensional vector

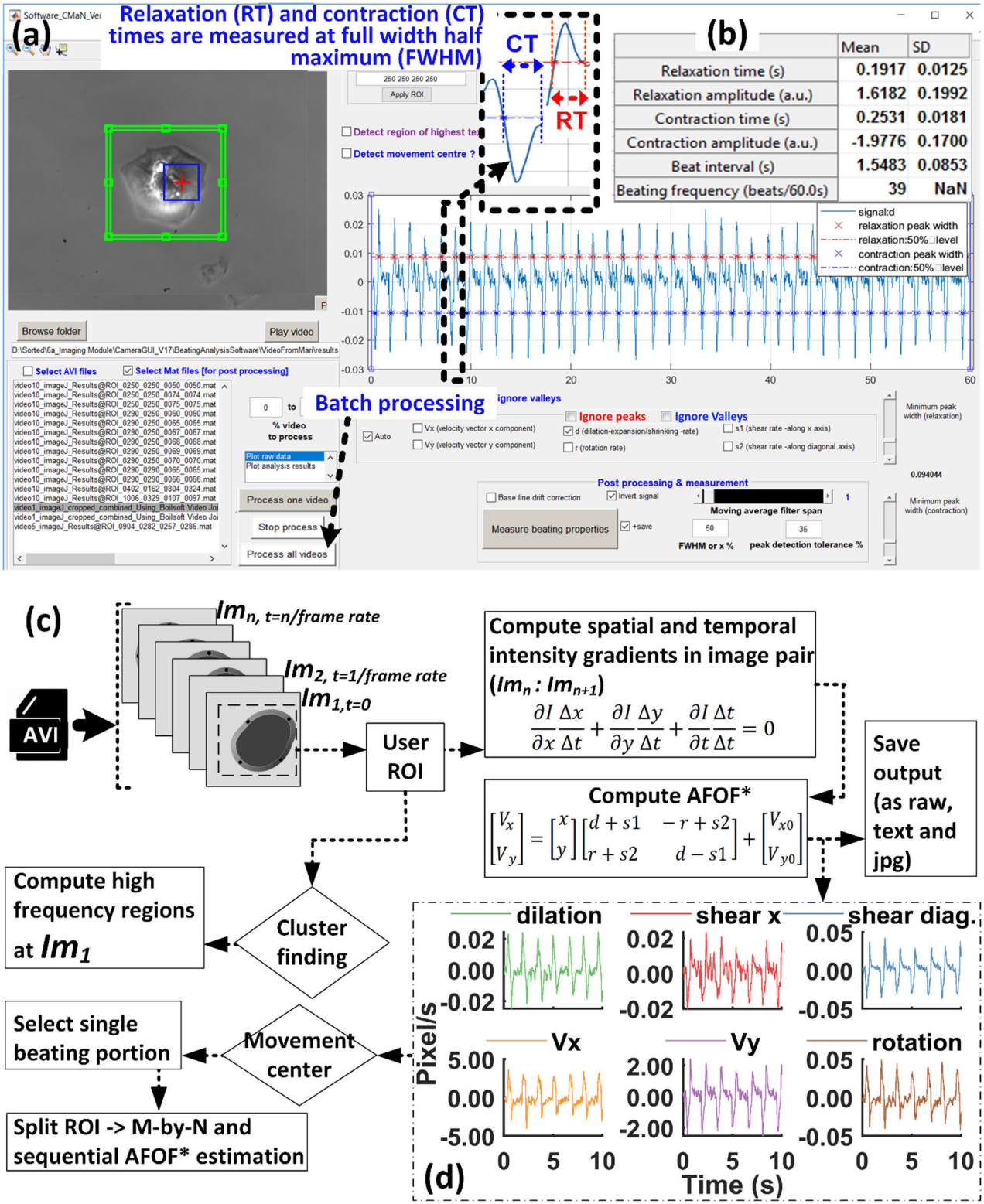

FIGURE 2. Advanced video-based movement analysis software, CMaN (Cardiomyocyte function analysis tool). (a) Screenshot from the software user interface. In the upper left corner, the blue rectangle shows the movement center of a single-cell CM, whereas the green rectangle shows the user-selected ROI. (b) Table of the estimated mechanobiology parameters. (c) A schematic overview of the algorithm flow and the principle behind the *AFOF (affine optical flow) computation from image pairs. (d) Six signal components of the contractile motion extracted from a single cell beating video.

to describe the x and y translation velocities (V_x, V_y), dilation, i.e., the rate of expansion/shrinking (d), the rate of rotation around the z axis (r), and the shear rates along the x axis (s1) and the main diagonal (s2). These six parameters are estimated by computing the least squares on the spatial and temporal gray-level gradients in consecutive video frames [43], [44]. FIGURE 2a shows a screenshot of CMaN. The six signal components analyzed from an example single cell are shown in FIGURE 2c,d. Several mechanobiological [32], [37], [46] parameters, namely, the beating frequency, relaxation time, contraction time, amplitude of beating, and beat-to-beat interval, can be estimated using one or more of the six signals. FIGURE 2b shows a table of these parameters analyzed from a single cell. Beating of both single cells and large clusters can be analyzed independently or batchwise. TABLE 1 summarizes the performance of CMaN compared with MUSCLEMOTION (v1-1beta.ijm) and SarcTrack (v 2019). See [47], and FIGURE 4 shows a comparison of their measurement sensitivities. CMaN has already been applied elsewhere [48] for CM tracking in conductive hyaluronic acid hydrogels. Additionally, example drug response plots of beat rate increasing and decreasing drugs that was analyzed with CMaN is provided in Supplementary Material 4 [49], [50].

D. MOVEMENT CENTER DETECTION AND CLUSTER FINDING

One novel feature of CMaN is movement center detection, which identifies the location of the most energetic movement area by detecting the region of the highest affine flow signal amplitude. This feature is illustrated in FIGURE 3a–b. The computation starts with a short portion of the beating signal containing at least one contraction–relaxation segment. Each image (either full frame or ROI) in the selected portion is first spatially sampled into M-by-N tiles (FIGURE 3b, where M and N are even). Then, the affine flow is sequentially computed in all the tiles, and the tile with the highest signal amplitude (movement center) is identified. In FIGURE 3a, the blue dashed rectangle shows the movement center identified over the user-selected ROI (green rectangle). An example of beating signals from the ROI and those separate from the identified movement center and the neighborhood are shown in Supplementary Material 5. One advantage of the movement center detection is that once the movement center is known, the best beating signal can be extracted by analyzing the area around the center.

The CMaN software also provides tools for finding CM clusters by identifying the locations of the highest textures (high-frequency regions), which is illustrated in FIGURE 3c. The cells in the CM cluster generate high-frequency textures (FIGURE 3c, left). First, the image is gamma corrected, smoothed, and low pass filtered, which results in bright cluster boards against a black background (FIGURE 3c, middle). This is followed by image convolution using a large-area template on the entire frame (full frame/ROI). Thus, multiple clusters can be distinguished from the surroundings. In FIGURE 3c, right, blue rectangles show three identified clusters. This feature provides a way to automate both cluster detection and beating analysis.

TABLE 2. Summary of temperature response experiments.

Cluster code	Temperature (range, step, [°C])	Number of replication cycles (code: RNo)	Logging interval TSP (minutes)	Logging interval Video (hours)
C1	37-25-37, 3	5	1	2
C2	37-25-37, 3	5	1	2
C3	37-25-37, 3	8	1	2
C4	37-25-37, 3	8	1	2
C5	37-25-37, 3	8	1	2
C6	37-25-37, 3	8	1	2
C7	37-25-37, 3	8	1	2
C8	37-25-37, 3	8	1	2
C9	37-25-37, 3	6	1	2
C10	37-25-37, 3	6	1	2
C11	37-25-37, 3	4	1	2
C12	37-25-37, 3	2	1	2
C11	constant 37	-	1	4
C9	constant 37	-	1	18

E. EXPERIMENTAL PROTOCOLS

The culturing temperature was programmatically adjusted from 37°C to 25°C and back to 37°C in 3°C steps, and beating videos were recorded. Overall, twelve CM clusters were studied in five separate cell cultures; see TABLE 2 for the experimental summary. The temperature was logged every 60 s, and videos were logged every 2 h. When a new temperature was set, the culture was allowed to stabilize for 30 min before video logging. The results are provided in the **Automated temperature stressing** section. Contractile synchronization measurements were performed using cultures containing dissociated clusters, and the results from a six cluster case are provided in the **Contractile synchronization of dissociated hiPSC-CM clusters** section. Furthermore, plots of the temporal reduction in beating frequency for the cases of two long-term cultures are provided in the **Temporal changes in beating at a constant temperature** section. The Q_{10} temperature coefficients were calculated using an exponential model, $(BF_1/\ BF_2)^*\ \exp(10\ /\ [T_1 - T_2])$, where BF_1 and BF_2 are the beating frequencies at temperatures T_1 and T_2 [27]. **Statistical analysis:** Pairwise comparisons of the mean parameter values at different temperatures were performed using a one-sided parametric t-test, and $p < 0.05$ was regarded as statistically significant.

III. RESULTS

A. AUTOMATED TEMPERATURE STRESSING

The beating signals (V_y) analyzed from a representative cluster (C12, RNo-2) at three selected temperatures (37°C, 31°C, and 25°C) as an overlay on the corresponding beating videos are shown in FIGURE 5. Additionally, the figure displays the calculated values for the beating frequency (BF), contraction time (CT), relaxation time (RT), and relaxed time (RxT, the time between relaxation and contraction).

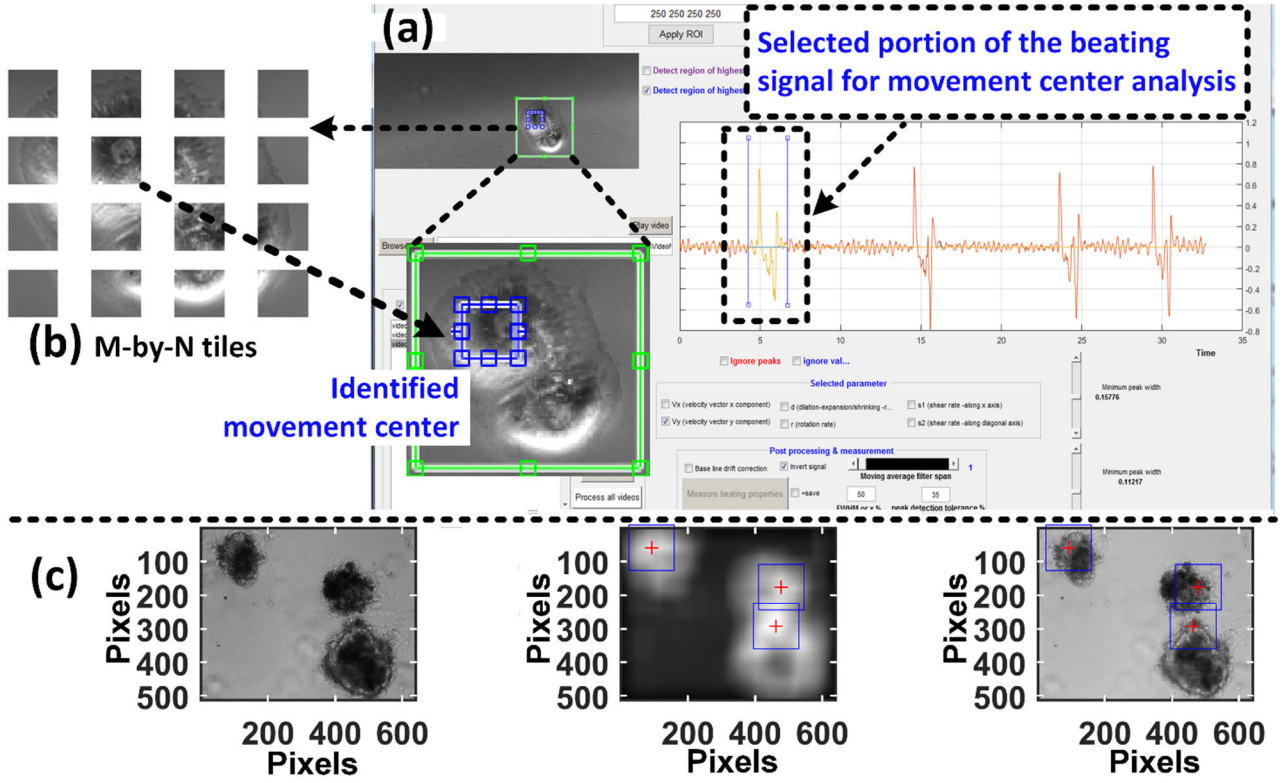

FIGURE 3. Movement center detection and cluster finding. (a, b) The signal portion of a contractionrelaxation region of a single cell selected for movement center analysis. The frames from this portion were spatially split into M-by-N tiles for sequential affine flow processing. The detected movement center is marked with a blue dashed rectangle. (c) Three images (first frame, smoothed, and with identified clusters) from the cluster-finding feature. The blue rectangles show the identified clusters in the *entire frame. See also* Supplementary Material 5.

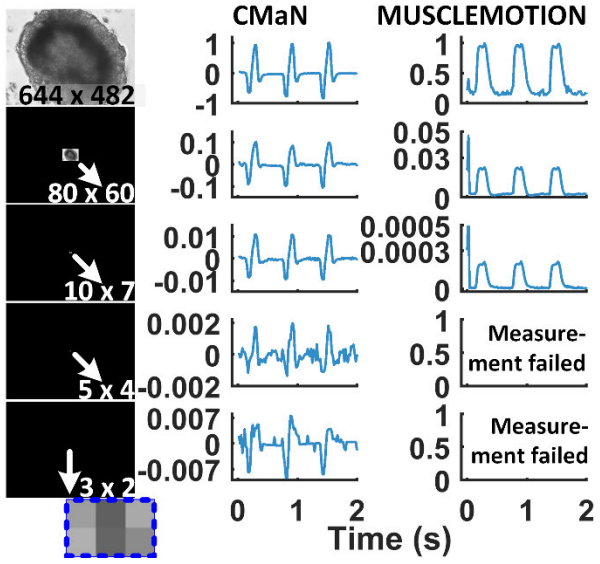

FIGURE 4. CMaN analysis sensitivity. Column 1: Screenshots of five videos. The original video (1st one) was spatially downsized 1/8, 1/64, 1/128, and 1/256 times to produce subsequent videos with a reduced movement area. Columns 2 & 3: Normalized signals (referenced to original signal, ROI: full frame, which also includes the black area in the downsized videos) analyzed with CMaN and MUSCLEMOTION. CMaN displayed better sensitivity.

The results show that lowering the temperature decreases BF and increases RT and RxT, whereas CT remains relatively constant. The full video is provided in Supplementary Material 2. FIGURE 6a–e show the temperature-induced changes in the beating frequency (BF), contraction time (CT), relaxation time (RT), and amplitude of contraction for two representative clusters (C9, C10, RNo-1:4). The data are from four consecutive stressing cycles over approximately 60 h. The results show that hiPSC-CM contractility responds strongly to temperature changes: the beating frequency (FIGURE 6b) changes proportionally to temperature and declines over time (see also FIGURE 7b, C9 and C10, ∼100 h). For a single representative stressing cycle (FIGURE 7a, C12, RNo-1), the linear temperature coefficient was approximately 5 BPM/°C (the coefficient of determination, R^2 = 0.97). Remarkably, nonlinear functions provide better fits, e.g., a 2nd degree polynomial and a mono-exponential function yielded R^2 = 0.9999 and R^2 = 0.9996, respectively. FIGURE 7c shows the beating frequency (C9, C10) combined with their nonlinear fits for 60 h of culture. The Q_{10} temperature coefficients (see plots) were larger than 2, implying a strong temperature dependence. Additionally, the R^2 of the nonlinear fits (FIGURE 7d) are typically larger than those of linear (poly1) fits.

Furthermore, the nonlinear temperature dependence was confirmed in the case of all 12 clusters, and its significance was statistically verified with the t-test on the R^2 values. The nonlinear R^2 > linear R^2 for 0–15 h (means of 93%

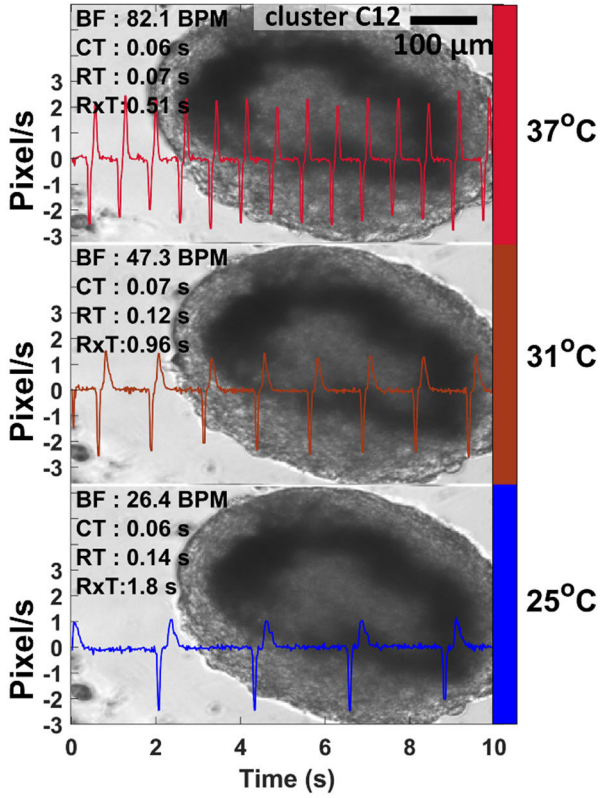

FIGURE 5. Effect of temperature on hiPSC-CM function. We show the analyzed beating signals (C12, RNo-1) at three selected temperatures as an overlay on the corresponding videos. See Supplementary Material 2 for the full video. Calculated values are shown for the beating frequency (BF), contraction time (CT), relaxation time (RT), and relaxed time (RxT, the time between relaxation and contraction).

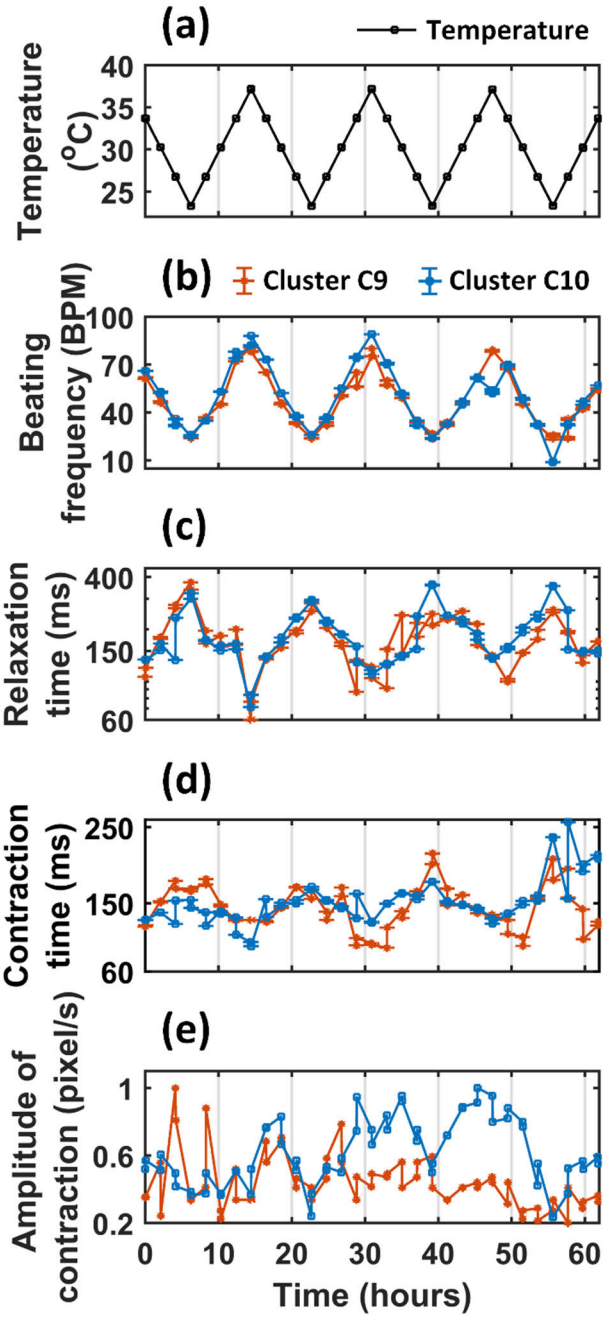

FIGURE 6. Temperature response plots of the two representative hiPSC-CM clusters (C9 and C10). Experimental data from approximately 60 h of mechanobiological measurements of (a) cell area temperature, (b) beating frequency, (c) contraction time, (d) relaxation time, and (e) amplitude of contraction. The temperature was precisely measured using the temperature-sensitive plate, and the plotted parameters were non-invasively analyzed using the video-based beating analysis software, CMaN.

and 90%, $p < 0.05$) and 0–30 h (means of 91% and 88%, $p < 0.05$). However, for durations > 30 h, several clusters showed a reduction in spontaneous contractility by factors other than temperature; hence, the statistical analysis can become complex.

Similarly, the contraction and relaxation times also vary but inversely (see FIGURE 6c, d) with temperature; thus, their magnitudes are larger at lower temperatures. Additionally, the relaxation times were larger than the contraction times. In TABLE 3, the relaxation and contraction times at low ($T = 25.0 \pm 0.1$°C) and high ($T = 37.1 \pm 0.1$°C) temperatures are provided. They show that a 12°C decline in temperature causes an 80% increase in contraction time and a 115% increase in relaxation time. Similarly, the contraction amplitude (FIGURE 6e), calculated as the geometric mean of amplitudes of V_x and V_y signals, also showed a strong temperature dependence similar to the beating frequency. However, the beat-to-beat amplitude variation in the 60-s videos, especially at low temperatures, was large.

Additionally, the beating frequency from four stress cycles for all twelve clusters (from five different cell cultures) is shown in FIGURE 8. The range of the beating frequency varied from culture to culture; for statistical comparison, frequencies were scaled between 1 and 0 using a normalization function (BF − min(BF)) / (max(BF) − min(BF)), where BF is the beating frequency. Despite the normalization, the error bars show relatively large variations, which presumably resulted from the biological variability between the individual clusters.

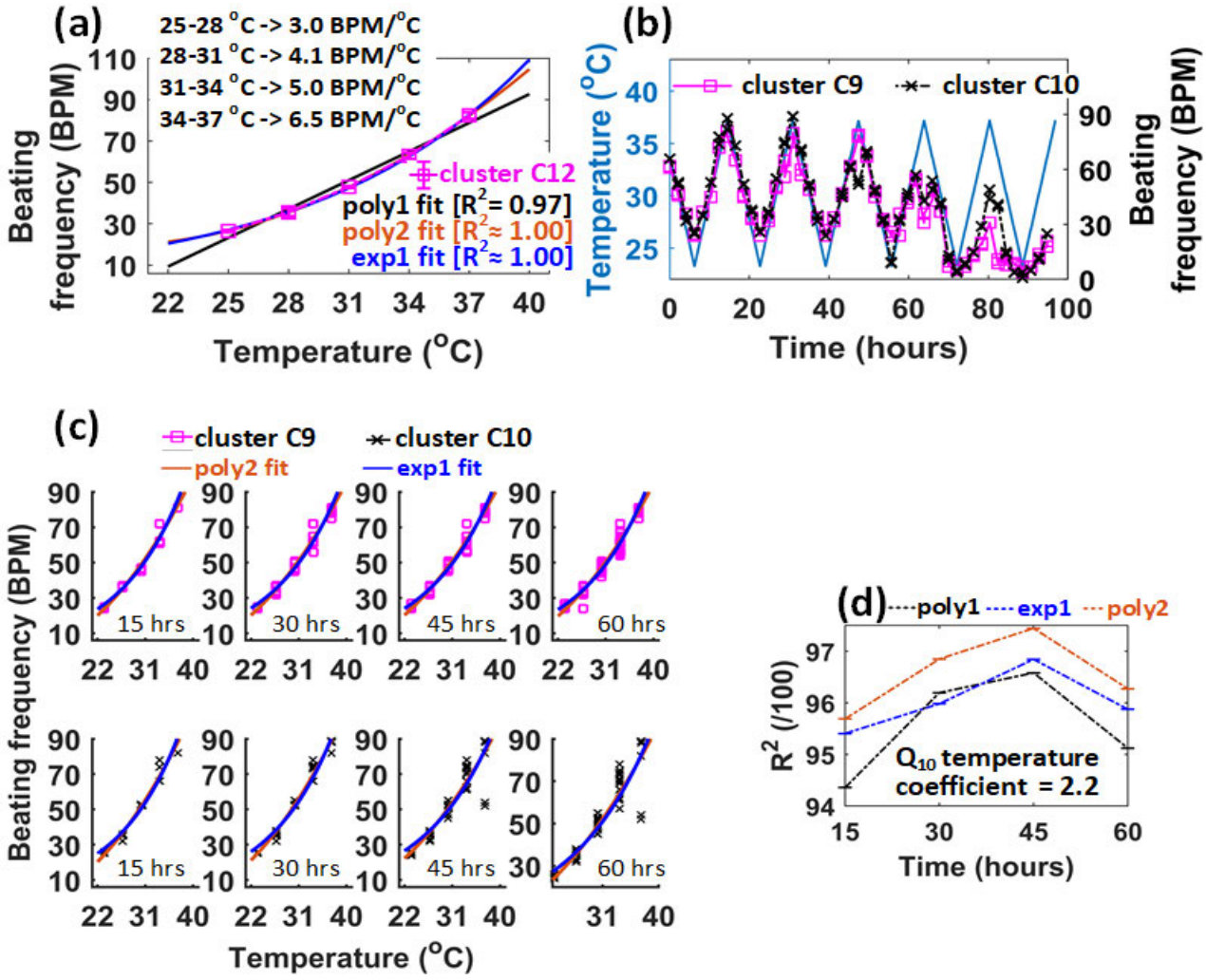

FIGURE 7. The hiPSC-CM beating frequency in long-term temperature stressing experiments. The data are from automated temperature cycles of decreasing (37°C to 25°C) and increasing (25°C to 37°C) temperatures in 3°C steps. (a) C12 data from a representative single stressing cycle (RNo-1) with linear and nonlinear (polynomial 2 and mono-exponential) fits. Compared to the linear fit, the nonlinear functions showed nearly perfect ($R^2 \approx 1$) fits. (b) Beating frequencies of two clusters (C9 and C10, RNo-1:4) over approximately 60 h of experiment. (c) Data (shown in upper right figure) rearranged into different time segments with 2^{nd} degree polynomial and mono-exponential fits. The computed Q_{10} temperature coefficients are shown in each figure, showing a strong temperature dependence on the hiPSC-CM function. However, the coefficient of determination decreased significantly in extended cultures.

TABLE 3. Mean relaxation and contraction times for all clusters (C1-C12) at the two temperatures. Results are presented in terms of means and standard deviations. Statistical analysis was performed according to a t-test (one-tailed). Statistical significances are denoted as * $p < 0.05$ and ** $p < 0.01$.

Temperature (°C)	Contraction time (CT, ms)		Relaxation time(RT, ms)		RT to CT ratio
37.1 ± 0.1	152 ± 21.6	**	177.3 ± 55.6	*	1.1
25.0 ± 0.1	274.1 ± 93.4		367.0 ± 110		1.3

B. CONTRACTILE SYNCHRONIZATION OF DISSOCIATED hiPSC-CM CLUSTERS

We also quantified the electrical activation (AP propagation) between dissociated clusters by measuring the time delay between their beatings. FIGURE 10a shows six beating clusters (C3 to C8), and their movement centers are marked with blue rectangles. Their beating signals are shown in FIGURE 10c, where the AP propagation time delay between contractions is clear. The signal propagation was also made visually detectable in the original video by image processing; an example video is provided in Supplementary Material 3. FIGURE 10b shows selected frames from this video. The dynamic sequence of cluster networking started at the cluster 3 (FIGURE 10b(i)) and passed through other clusters up until cluster 6 (FIGURE 10b(vi)). Each frame was produced as the absolute difference in intensity between the actual frame and the first frame. As a result, a brighter passing halo became visible to describe the AP propagation delay. In FIGURE 10d, this time delay is plotted as a function of the cluster distance (cluster X – cluster C3, where X is C8 or C7 or C6 or C5 or C4 or C3), and the corresponding AP propagation velocities (slope) were calculated to be $v = 3.88$, 2.76, 2.34, and 1.98 mm/s at T = 37, 34, 31, and 28°C, respectively.

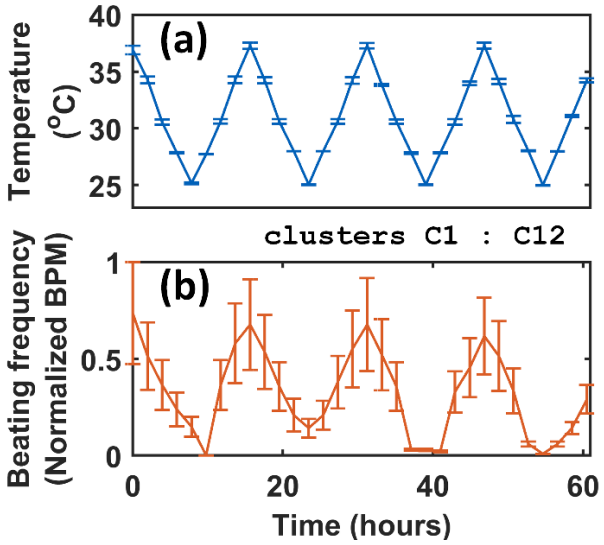

FIGURE 8. Beating frequency of twelve spontaneously beating hiPSC-CM clusters during four stress cycles. The clusters are from five different cell cultures in which the range of beating frequency varied from culture to culture. Thus, the error bars also account for the biological variability.

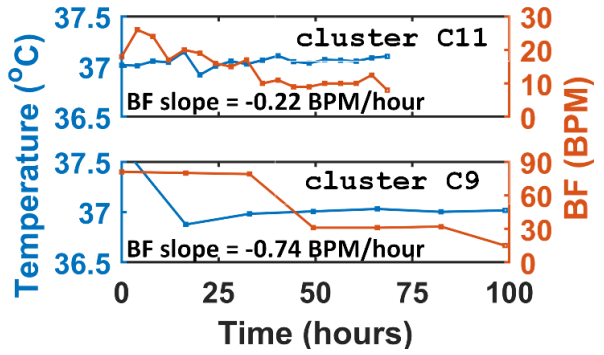

FIGURE 9. Temporal reduction of beating frequency at 37°C in two separate cultures. A 68-85% decline in beating frequency was observed over 70-100 h.

C. TEMPORAL CHANGES IN BEATING AT A CONSTANT TEMPERATURE

Additionally, the contractility slowly decreased over extended time periods even at a constant temperature. The beating frequency plots from two long-term measurements at a constant 37°C with 2 clusters (C11, C9) are shown in FIGURE 9. The measured slope (dBF / dt [BPM/h]) values are −0.22 and −0.74, respectively, indicating a 68%–85% decline in beating frequency over 70–100 h. The decline rate likely depends on many factors, including cell density, secretory/metabolic conditions, and medium aging (exhaustion of accessory food factors).

IV. DISCUSSION

Herein, we demonstrated the applicability of a previously reported modular cell culturing system [26] with two new add-ons: 1) temperature sensor plates [24] and 2) novel video-based mechanobiology analysis software, CMaN, to study the temperature response of hiPSC-CMs. Experiments were conducted outside a conventional incubator, and to our knowledge, this is the first report describing a systematic automated temperature stress test and concurrent hiPSC-CM function analysis. Results showed that the hiPSC-CM contractile function is strongly temperature dependent and that typically the temperature coefficient is $Q_{10} > 2$. Additionally, the beating frequency–temperature relationship was described by nonlinear (2^{nd} order polynomial and mono-exponential) functions. In the statistical analysis, the R^2 values were always higher for nonlinear models than for linear ones, and some clusters showed nearly perfect ($R^2 \sim 1$) nonlinear fits. Thus, maintaining a stable temperature during hiPSC-CMs experiments is crucial to minimize undesired stimulation of cells and avoid experimental errors. Moreover, during continuous measurements, the contractility of the hiPSC-CMs decreased with time even at fixed temperatures, which is also an important factor to consider for experimental designs. The medium aging, evaporation, and related changes in the medium composition as well as the exhaustion of essential nutrients likely contribute to the slowing of the contractile kinetics temporally [19]. The combined beating frequency plot (FIGURE 8) shows data from twelve beating clusters from five different cell cultures; thus, the error bars also account for the biological variability. Because hiPSC-CMs are known to exhibit a high phenotype variability, the variability of the temperature dependency between different myocytes/culture preparations must also be considered. In contrast to the beating frequency, the contraction and relaxation times inversely vary with temperature. The relaxation times are typically longer than the contraction times. The contraction amplitude, however, displayed more beat-to-beat variability (standard deviation) in almost all recorded videos. Interestingly, some clusters occasionally ceased the beating function but regained the function slowly and exhibited a temperature dependence during continued stress cycles.

Biologically, the temperature dependence of hiPSC-CMs can be multifactorial. A more general explanation is the prolongation of APs at lower temperatures due to slower kinetics of underlying ion channels, exchangers, and intracellular pumps [51]. The hiPSC-CMs, which are similar to their native human counterparts, have most of the basic underlying excitation–contraction coupling components, including membrane voltage regulation and signaling cascades [52]–[54]. However, reduced inward rectifier K^+ (potassium) currents and presence of prominent pacemaker currents collectively produce AP waveforms that make hiPSC-CMs significantly different and facilitate spontaneous automaticity not observed in mature human ventricular myocytes [53]. Temperature dependence of AP prolongation has been previously studied in animal models [55], [56]. Guinea pig ventricular myocytes have shown 115% prolongation of AP with 10°C temperature decrease [56]. The acute effect of temperature on the relaxation time and pacemaker firing rate of Sprague–Dawley rat CMs has also been reported [3]. Herein, we systematically measured the prolongation of hiPSC-CM relaxation

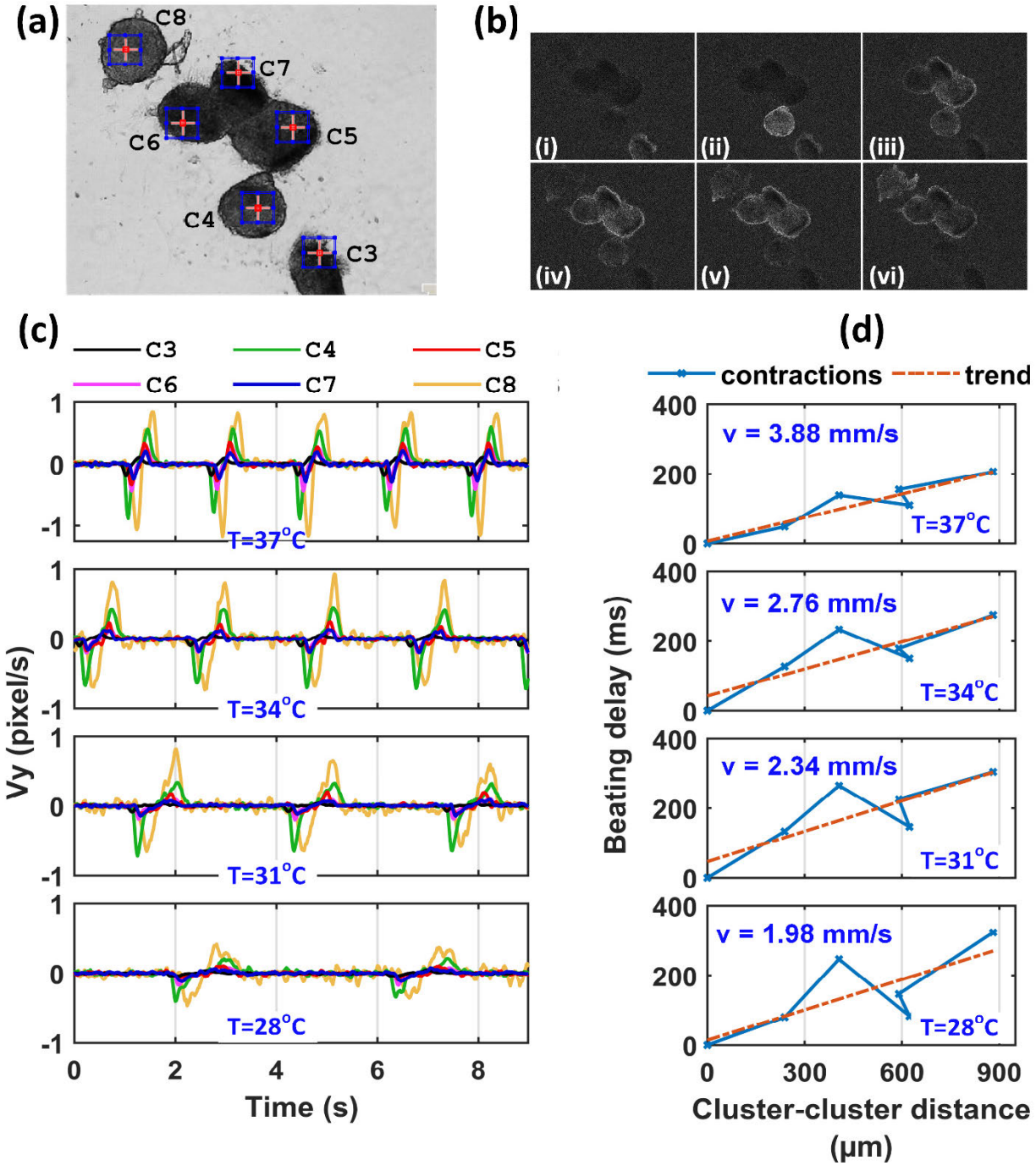

FIGURE 10. Contractile synchronization of dissociated hiPSC-CM clusters. (a) Six beating clusters, where the blue rectangles show their movement centers analyzed with CMaN. The action potential (AP) signal propagation between dissociated clusters became observable in the original video upon image processing. See Supplementary Material 3 for an example video. (b) Selected frames from Supplementary Material 3, where a passing brighter halo displays the AP propagation. The networking dynamic sequence starts from cluster 1 and advances up to cluster 6. (c) Beating signals from the six clusters, where the time delay between the signals is clear. (d) The time delay versus the cluster separation distance (cluster X – cluster C3, where X is C8 or C7 or C6 or C5 or C4 or C3) plots and the computed AP propagation velocities.

(analogue to the AP repolarization) and contraction times. Multiple voltage-gated ion channels presumably contribute to this; however, the exact quantification schemes of the dependence of most of the underlying mechanisms on environmental parameters (e.g., temperature, pO_2, pH, osmolarity and pCO_2) are ambiguous, and accurate models have not yet been developed.

We also measured the propagation of electrical activation between dissociated hiPSC-CM clusters using optical methods. The clusters, although physically separated, are

possibly connected to each other via cells (non-CMs) underneath, which act as a cardiac skeleton for mechanical scaffolding. Few studies using animal cells have confirmed the electrophysiological coupling of fibroblasts (of cardiac origin) with CMs to propagate contractions over finite distances [57]–[59]. Recently, some studies quantified the AP propagation distance and beating synchronization of certain CM types [7], [60], [61]. Herein, we quantified the synchronization delay for hiPSC-CMs using non-invasive image-based measurements and measured the AP propagation velocities (v = 1.98–3.88 mm/s at 28–37°C). The AP propagation velocities can obviously be a function of cell density, configuration (single cells, cell sheets, etc.), age, and maturation state.

The software, CMaN, is freely available and in contrast to compared software programs, it is several times faster, more robust and sensitive, computationally less expensive, and allows easy ROI selection. This allows careful processing of specific areas/cells, for instance when frames contain multiple cells/clusters. Furthermore, CMaN extracts six components of contractile motion per processing, enabling a minimum of one useful beating signal even in complex scenarios, such as weak movements or overexposure/gamma by uneven background illumination. The signal from CMaN is analogous to ECG with both positive (upstroke) and negative (downstroke) segments that represent the contractile phenomena more exactly. This helps compute the beating frequency and contraction and relaxation phenomena separately. Additionally, CMaN has supplemental features for cluster finding and movement center detection. One limitation of CMaN is that it can currently only process avi files. If the input comes as a sequence of images, those have to be first converted into an avi file (for example using ImageJ or the script provided in the CMaN user manual). Currently, the mechanobiological analysis is performed in two stages: the first stage is the automatic signal extraction, and in the second stage, fine tuning (adjusting thresholds with sliders in GUI) may be required in the case of heavily noisy or complex beating scenarios. The software is an offline tool; however, the basic script for the affine flow computation is provided (see CMaN user manual), which can be edited for online automated beating analysis or other extended applications. One future direction is the measurement of contractile forces with beating signals by integrating a micro-displacement actuator (e.g., fluorescent beads, magnetic beads, micro-cantilevers). We are also developing cell and disease models in which the platform described herein is directly applied.

V. CONCLUSIONS

We have described a system and software that allows the assessment of hiPSC derived CM contractions with changing temperatures. The highlights of the paper include the first reporting of 1) the nonlinear temperature dependence on the beating frequency of hiPSC-CMs, 2) the visualization of hiPSC-CM contractile networking and the non-invasive measurement of signal propagation between dissociated clusters, and 3) the release of an advanced and robust software that tracks multiple signals from CM beating videos. The system and software are useful additions to assay development and organ-on-chip experiments.

CONFLICT OF INTERESTS

The authors report no conflicts of interest.

REFERENCES

[1] R. Madonna, "Human-induced pluripotent stem cells: In quest of clinical applications," *Mol. Biotechnol.*, vol. 52, no. 2, pp. 193–203, Oct. 2012.

[2] V. K. Singh, M. Kalsan, N. Kumar, A. Saini, and R. Chandra, "Induced pluripotent stem cells: Applications in regenerative medicine, disease modeling, and drug discovery," *Frontiers Cell Develop. Biol.*, vol. 3, p. 2, Feb. 2015.

[3] C. S. Chung and K. S. Campbell, "Temperature and transmural region influence functional measurements in unloaded left ventricular cardiomyocytes," *Physiol. Rep.*, vol. 1, no. 6, pp. 1–13, 2013.

[4] C. G. Crandall and J. González-Alonso, "Cardiovascular function in the heat-stressed human," *Acta Physiologica*, vol. 199, no. 4, pp. 407–423, Aug. 2010.

[5] T. E. Wilson and C. G. Crandall, "Effect of thermal stress on cardiac function," *Exercise Sport Sci. Rev.*, vol. 39, no. 1, pp. 12–17, Jan. 2011.

[6] K. B. Storey and J. M. Storey, "Mammalian hibernation: Biochemical adaptation and gene expression," in *Functional Metabolism: Regulation and Adaptation*. Hoboken, NJ, USA: Wiley, 2005, pp. 443–471.

[7] R. Kienast, M. Stöger, M. Handler, F. Hanser, and C. Baumgartner, "Alterations of field potentials in isotropic cardiomyocyte cell layers induced by multiple endogenous pacemakers under normal and hypothermal conditions," *Amer. J. Physiol.-Heart Circulatory Physiol.*, vol. 307, no. 7, pp. H1013–H1023, Oct. 2014.

[8] H. Orita, M. Fukasawa, S. Hirooka, K. Fukui, M. Kohi, and M. Washio, "A cardiac myocyte culture system as an *in vitro* experimental model for the evaluation of hypothermic preservation," *Surgery Today*, vol. 23, no. 5, pp. 439–443, May 1993.

[9] K. E. Cullen and K. D. Sarge, "Characterization of hypothermia-induced cellular stress response in mouse tissues," *J. Biol. Chem.*, vol. 272, no. 3, pp. 1742–1746, Jan. 1997.

[10] A. Stolzing, S. Sethe, and A. M. Scutt, "Stem cell reports," *Stem Cells Dev.*, vol. 15, no. 4, pp. 478–487, Aug. 2006.

[11] K. Purandhar, P. K. Jena, B. Prajapati, P. Rajput, and S. Seshadri, "Understanding the role of heat shock protein isoforms in male fertility, aging and apoptosis," *World J. Men's Health*, vol. 32, no. 3, p. 123, Dec. 2014.

[12] M. S. Choudhery, M. Khan, R. Mahmood, S. Mohsin, S. Akhtar, F. Ali, S. N. Khan, and S. Riazuddin, "Mesenchymal stem cells conditioned with glucose depletion augments their ability to repair-infarcted myocardium," *J. Cellular Mol. Med.*, vol. 16, no. 10, pp. 2518–2529, Oct. 2012.

[13] J. Kockskämper, "Excitation–contraction coupling of cardiomyocytes," in *Cardiomyocytes–Active Players in Cardiac Disease*. Cham, Switzerland: Springer, 2016, pp. 67–96.

[14] N. Schaible, Y. S. Han, T. Hoang, G. Arteaga, T. Tveita, and G. Sieck, "Hypothermia/rewarming disrupts excitation-contraction coupling in cardiomyocytes," *Amer. J. Physiol.-Heart Circulatory Physiol.*, vol. 310, no. 11, pp. H1533–H1540, Jun. 2016.

[15] B. D. Stuyvers, A. D. McCulloch, J. Guo, H. J. Duff, and H. E. D. J. Ter Keurs, "Effect of stimulation rate, sarcomere length and Ca^{2+} on force generation by mouse cardiac muscle," *J. Physiol.*, vol. 544, no. 3, pp. 817–830, Nov. 2002.

[16] T. Tveita, M. Skandfer, H. Refsum, and K. Ytrehus, "Experimental hypothermia and rewarming: Changes in mechanical function and metabolism of rat hearts," *J. Appl. Physiol.*, vol. 80, no. 1, pp. 291–297, Jan. 1996.

[17] J. A. Ryan. (2019). *Corning Guide for Identifying and Correcting Common Cell Growth Problems*. Corning Incorporated Life Sciences. Accessed: Jan. 12, 2017. [Online]. Available: https://beta-static.fishersci.com/content/dam/fishersci/en_US/documents/programs/scientific/technical-documents/technical-bulletins/corning-guide-identifying-cell-growth-problems-technical-bulletin

[18] D. K. Rajan, J. Verho, J. Kreutzer, H. Välimäki, H. Ihalainen, J. Lekkala, M. Patrikoski, and S. Miettinen, "Monitoring pH, temperature and humidity in long-term stem cell culture in CO_2 incubator," in *Proc. IEEE Int. Symp. Med. Meas. Appl. (MeMeA)*, May 2017, pp. 470–474.
[19] F. Wang, "Culture of animal cells: A manual of basic technique, fifth edition," *Vitro Cellular Develop. Biol. Animal*, vol. 42, no. 5, p. 169, 2006.
[20] D. Kattipparambil Rajan, M. Patrikoski, J. Verho, J. Sivula, H. Ihalainen, S. Miettinen, and J. Lekkala, "Optical non-contact pH measurement in cell culture with sterilizable, modular parts," *Talanta*, vol. 161, pp. 755–761, Dec. 2016.
[21] J. Kreutzer, L. Ylä-Outinen, A.-J. Mäki, M. Ristola, S. Narkilahti, and P. Kallio, "Cell culture chamber with gas supply for prolonged recording of human neuronal cells on microelectrode array," *J. Neurosci. Methods*, vol. 280, pp. 27–35, Mar. 2017.
[22] S. Fulda, A. M. Gorman, O. Hori, and A. Samali, "Cellular stress responses: Cell survival and cell death," *Int. J. Cell Biol.*, vol. 2010, Feb. 2010, Art. no. 214074.
[23] E. Laurila, A. Ahola, J. Hyttinen, and K. Aalto-Setälä, "Methods for *in vitro* functional analysis of iPSC derived cardiomyocytes—Special focus on analyzing the mechanical beating behavior," *Biochimica et Biophysica Acta, Mol. Cell Res.*, vol. 1863, no. 7, pp. 1864–1872, Jul. 2016.
[24] A.-J. Mäki, J. Verho, J. Kreutzer, T. Ryynänen, D. Rajan, M. Pekkanen-Mattila, A. Ahola, J. Hyttinen, K. Aalto-Setälä, J. Lekkala, and P. Kallio, "A portable microscale cell culture system with indirect temperature control," *SLAS Technology, Translating Life Sci. Innov.*, vol. 23, no. 6, pp. 566–579, Dec. 2018.
[25] T. Uchida, R. Kitora, and K. Gohara, "Temperature dependence of synchronized beating of cultured neonatal rat heart-cell networks with increasing age measured by multi-electrode arrays," *Trends Med.*, vol. 18, no. 4, pp. 1–10, 2018.
[26] D. K. Rajan, J. Kreutzer, H. Valimaki, M. Pekkanen-Mattila, A. Ahola, A. Skogberg, K. Aalto-Setala, H. Ihalainen, P. Kallio, and J. Lekkala, "A portable live-cell imaging system with an invert-upright-convertible architecture and a mini-bioreactor for long-term simultaneous cell imaging, chemical sensing, and electrophysiological recording," *IEEE Access*, vol. 6, pp. 11063–11075, 2018.
[27] M. K. Worden, C. M. Clark, M. Conaway, and S. A. Qadri, "Temperature dependence of cardiac performance in the lobster Homarus americanus," *J. Express Biol.*, vol. 209, no. 6, pp. 1024–1034, Mar. 2006.
[28] G. Caluori, J. Pribyl, V. Cmiel, M. Pesl, T. Potocnak, I. Provaznik, P. Skladal, and V. Rotrekl, "Simultaneous study of mechanobiology and calcium dynamics on hESC-derived cardiomyocytes clusters," *J. Mol. Recognit.*, vol. 32, no. 2, p. e2760, Feb. 2019.
[29] S. Dinarelli, M. Girasole, P. Spitalieri, R. V. Talarico, M. Murdocca, A. Botta, G. Novelli, R. Mango, F. Sangiuolo, and G. Longo, "AFM nanomechanical study of the beating profile of hiPSC-derived cardiomyocytes beating bodies WT and DM1," *J. Mol. Recognit.*, vol. 31, no. 10, p. e2725, Oct. 2018.
[30] M. Pesl, J. Pribyl, G. Caluori, V. Cmiel, I. Acimovic, S. Jelinkova, P. Dvorak, Z. Starek, P. Skladal, and V. Rotrekl, "Phenotypic assays for analyses of pluripotent stem cell-derived cardiomyocytes," *J. Mol. Recognit.*, vol. 30, no. 6, p. e2602, Jun. 2017.
[31] P. Spitalieri, R. V. Talarico, S. Caioli, M. Murdocca, A. Serafino, M. Girasole, S. Dinarelli, G. Longo, S. Pucci, A. Botta, G. Novelli, C. Zona, R. Mango, and F. Sangiuolo, "Modelling the pathogenesis of myotonic dystrophy type 1 cardiac phenotype through human iPSC-derived cardiomyocytes," *J. Mol. Cellular Cardiol.*, vol. 118, pp. 95–109, May 2018.
[32] A. Ahola, A. L. Kiviaho, K. Larsson, M. Honkanen, K. Aalto-Setälä, and J. Hyttinen, "Video image-based analysis of single human induced pluripotent stem cell derived cardiomyocyte beating dynamics using digital image correlation," *Biomed. Eng. OnLine*, vol. 13, no. 1, p. 39, 2014.
[33] C. L. Mummery, B. J. Van Meer, L. G. J. Tertoolen, J. Bakkers, M. Bellin, R. P. Davis, C. Denning, M. A. Dieben, T. Eschenhagen, E. Giacomelli, and C. Grandela, "MUSCLEMOTION: A versatile open software tool to quantify cardiomyocyte and cardiac muscle contraction *in vitro* and *in vivo*," *Circulat. Res.*, vol. 122, no. 3, pp. e5–e16, 2017.
[34] C. N. Toepfer, A. Sharma, M. Cicconet, A. C. Garfinkel, M. Mücke, M. Neyazi, J. A. L. Willcox, R. Agarwal, M. Schmid, J. Rao, J. Ewoldt, O. Pourquié, A. Chopra, C. S. Chen, J. G. Seidman, and C. E. Seidman, "SarcTrack: An adaptable software tool for efficient large-scale analysis of sarcomere function in hiPSC-cardiomyocytes," *Circulat. Res.*, vol. 124, no. 8, pp. 1172–1183, Apr. 2019.
[35] S. Nitsch, F. Braun, S. Ritter, M. Scholz, and I. S. Schroeder, "Functional video-based analysis of 3D cardiac structures generated from human embryonic stem cells," *Stem Cell Res.*, vol. 29, pp. 115–124, May 2018.
[36] M. Maddah, J. D. Heidmann, M. A. Mandegar, C. D. Walker, S. Bolouki, B. R. Conklin, and K. E. Loewke, "A non-invasive platform for functional characterization of Stem-Cell-Derived cardiomyocytes with applications in cardiotoxicity testing," *Stem Cell Rep.*, vol. 4, no. 4, pp. 621–631, Apr. 2015.
[37] T. Hayakawa, T. Kunihiro, T. Ando, S. Kobayashi, E. Matsui, H. Yada, Y. Kanda, J. Kurokawa, and T. Furukawa, "Image-based evaluation of contraction–relaxation kinetics of human-induced pluripotent stem cell-derived cardiomyocytes: Correlation and complementarity with extracellular electrophysiology," *J. Mol. Cellular Cardiol.*, vol. 77, pp. 178–191, Dec. 2014.
[38] E. K. Lee, Y. K. Kurokawa, R. Tu, S. C. George, and M. Khine, "Machine learning plus optical flow: A simple and sensitive method to detect cardioactive drugs," *Sci. Rep.*, vol. 5, no. 1, p. 11817, Dec. 2015.
[39] J. Kreutzer, L. Ylä-Outinen, P. Kärnä, T. Kaarela, J. Mikkonen, H. Skottman, S. Narkilahti, and P. Kallio, "Structured PDMS chambers for enhanced human neuronal cell activity on MEA platforms," *J. Bionic Eng.*, vol. 9, no. 1, pp. 1–10, Mar. 2012.
[40] O. Metsälä, J. Kreutzer, H. Högel, P. Miikkulainen, P. Kallio, and P. M. Jaakkola, "Transportable system enabling multiple irradiation studies under simultaneous hypoxia *in vitro*," *Radiat. Oncol.*, vol. 13, no. 1, p. 220, Nov. 2018.
[41] A. L. Lahti, V. J. Kujala, H. Chapman, A.-P. Koivisto, M. Pekkanen-Mattila, E. Kerkelä, J. Hyttinen, K. Kontula, H. Swan, B. R. Conklin, and S. Yamanaka, "Model for long QT syndrome type 2 using human iPS cells demonstrates arrhythmogenic characteristics in cell culture," *Dis. Model. Mech.*, vol. 5, no. 2, pp. 220–330, Mar. 2012.
[42] C. Mummery, D. Ward-van Oostwaard, P. Doevendans, R. Spijker, S. van den Brink, R. Hassink, M. Van der Heyden, T. Opthof, M. Pera, A. B. de la Riviere, and R. Passier, "Differentiation of human embryonic stem cells to cardiomyocytes: Role of coculture with visceral endoderm-like cells," *Circulation*, vol. 107, no. 21, pp. 2733–2740, Jun. 2003.
[43] S. S. Beauchemin and J. L. Barron, "The computation of optical flow," *ACM Comput. Surv.*, vol. 27, no. 3, pp. 433–466, Sep. 1995.
[44] Y. David. (2010). *Affine Optic Flow (Version 1.3)*. MATLAB Central File Exchange. Accessed: Mar. 3, 2017. [Online]. Available: https://se.mathworks.com/matlabcentral/fileexchange/27093-affine-optic-flow
[45] C. Bonivento, C. Melchiorri, and H. Tolle, *Advances In Robotics: The Ernet Perspective-Proceedings Of The Research Workshop Of Ernet-European Robotics Network*. Darmstadt, Germany: World Scientific, 1996.
[46] J. Liu, N. Sun, M. A. Bruce, J. C. Wu, and M. J. Butte, "Atomic force mechanobiology of pluripotent stem cell-derived cardiomyocytes," *PLoS ONE*, vol. 7, no. 5, May 2012, Art. no. e37559.
[47] D. Rajan, "Modular instrumentation for controlling and monitoring *in-vitro* cultivation environment and image-based functionality measurements of human stem cells," DSc-Tech thesis, Tampere Univ., Tampere, Finland, 2020, vol. 256, pp. 1–150.
[48] H. Kemppi, "Gold nanoparticle crosslinked conductive hyaluronan and chondroitin sulfate hydrogels for culturing embryonic stem cells derived human cardiomyocytes," M.S. thesis, Tampere Univ., Tampere, Finland, 2018.
[49] D. Shah, L. Virtanen, C. Prajapati, M. Kiamehr, J. Gullmets, G. West, J. Kreutzer, M. Pekkanen-Mattila, T. Heliö, P. Kallio, P. Taimen, and K. Aalto-Setälä, "Modeling of LMNA-related dilated cardiomyopathy using human induced pluripotent stem cells," *Cells*, vol. 8, no. 6, p. 594, Jun. 2019.
[50] J. Kim, D. Shah, I. Potapov, J. Latukka, K. Aalto-Setälä, and E. Räsänen, "Scaling and correlation properties of RR and QT intervals at the cellular level," *Sci. Rep.*, vol. 9, no. 1, pp. 1–9, Dec. 2019.
[51] K. Wang, A. Climent, D. Gavaghan, P. Kohl, and C. Bollensdorff, "Room temperature vs ice cold-temperature effects on cardiac cell action potential," *Biophys. J.*, vol. 110, no. 3, p. 587a, Feb. 2016.
[52] C. Y. Ivashchenko, G. C. Pipes, I. M. Lozinskaya, "Human-induced pluripotent stem cell-derived cardiomyocytes exhibit temporal changes in phenotype," *Amer. J. Physiol. Hear. Circulatory Physiol.*, vol. 305, pp. 913–922, Sep. 2013.
[53] I. Karakikes, M. Ameen, V. Termglinchan, and J. C. Wu, "Human induced pluripotent stem cell–derived cardiomyocytes: Insights into molecular, cellular, and functional phenotypes," *Circulat. Res.*, vol. 117, no. 1, pp. 8–80, Jun. 2015.

[54] J. T. Koivumäki, N. Naumenko, T. Tuomainen, J. Takalo, M. Oksanen, K. A. Puttonen, Š. Lehtonen, J. Kuusisto, M. Laakso, J. Koistinaho, and P. Tavi, "Structural immaturity of human iPSC-derived cardiomyocytes: In silico investigation of effects on function and disease modeling," *Frontiers Physiol.*, vol. 9, p. 80, Feb. 2018.
[55] M. Laursen, S.-P. Olesen, M. Grunnet, T. Mow, and T. Jespersen, "Characterization of cardiac repolarization in the Göttingen minipig," *J. Pharmacological Toxicological Methods*, vol. 63, no. 2, pp. 186–195, Mar. 2011.
[56] T. Kiyosue, M. Arita, H. Muramatsu, A. J. Spindler, and D. Noble, "Ionic mechanisms of action potential prolongation at low temperature in guinea-pig ventricular myocytes," *J. Physiol.*, vol. 468, no. 1, pp. 85–106, Aug. 1993.
[57] T. Kaneko, F. Nomura, and K. Yasuda, "On-chip constructive cell-network study (I): Contribution of cardiac fibroblasts to cardiomyocyte beating synchronization and community effect," *J. Nanobiotechnol.*, vol. 9, no. 1, p. 21, May 2011.
[58] P. Kohl, "Heterogeneous cell coupling in the heart," *Circulat. Res.*, vol. 93, no. 5, pp. 381–383, Sep. 2003.
[59] G. Gaudesius, M. Miragoli, S. P. Thomas, and S. Rohr, "Coupling of cardiac electrical activity over extended distances by fibroblasts of cardiac origin," *Circulat. Res.*, vol. 93, no. 5, pp. 421–428, Sep. 2003.
[60] M. Miragoli, G. Gaudesius, and S. Rohr, "Electrotonic modulation of cardiac impulse conduction by myofibroblasts," *Circulat. Res.*, vol. 98, no. 6, pp. 801–810, Mar. 2006.
[61] J. P. Fahrenbach, R. Mejia-Alvarez, and K. Banach, "The relevance of non-excitable cells for cardiac pacemaker function," *J. Physiol.*, vol. 585, no. 2, pp. 565–578, Dec. 2007.

DHANESH KATTIPPARAMBIL RAJAN (Member, IEEE) received the M.Sc. (Tech.) degree from the Tampere University of Technology (TUT), Finland, in 2008, and the D.Sc. (Tech.) degree in biomedical engineering from Tampere University, Finland, in 2020. He has worked with photolithography techniques in TUT. He is involved in the development of portable cell culturing systems, modular microscopy, and optical and image-based measurements of human stem cell cultures.

ANTTI-JUHANA MÄKI received the M.S. degree in automation engineering from the Tampere University of Technology (TUT), Tampere, Finland, in 2010, and the Ph.D. degree in automation engineering from the Department of Automation Science and Engineering, in 2018, under the supervision of Prof. Kallio.

He is currently involved in the development of control system for automated human stem cell environment. His current research interests include control engineering, modeling, microfluidics, and autonomous systems for cell engineering.

MARI PEKKANEN-MATTILA (Member, IEEE) received the Ph.D. degree in stem cell and tissue engineering from the University of Tampere, Finland, in 2011. Her research interests include human induced pluripotent stem cells, cell differentiation, and disease modeling of human genetic cardiac diseases.

JOOSE KREUTZER received the B.Eng. degree in electrical and electronic engineering from the University of Sunderland, Sunderland, U.K., in 2003, and the M.Sc. degree in electrical engineering from the Tampere University of Technology (TUT), Tampere, Finland, in 2005. He currently works as a Research Scientist with the Micro and Nanosystems Research Group, BioMediTech Institute, and the Faculty of Biomedical Sciences and Engineering, TUT. His current research interests include microfabrication, microfluidics, and their applications in biomedical engineering, especially for stem cell-based bioengineering.

TOMI RYYNÄNEN received the M.Sc. degree in applied physics from the University of Jyväskylä, Finland, in 2000, and the Ph.D. degree in biomedical engineering from Tampere University, Finland, in 2019. His main research interests include in vitro microelectrode arrays (MEAs) and microfabrication.

HANNU VÄLIMÄKI received the M.Sc. degree in electrical engineering from the Tampere University of Technology (TUT), Tampere, Finland, in 1996. He has worked as a Research Scientist in the field of acoustical and optical sensors with the VTT Technical Research Centre of Finland, Tampere, until 2013. He currently works with the BioMediTech Institute and the Faculty of Biomedical Sciences and Engineering, TUT, where he develops optical sensing technologies for cell culturing applications.

JARMO VERHO is currently a Research Assistant with the Department of Automation Science and Engineering, Tampere University of Technology, Tampere, Finland. His current research interests include low-noise electronics design and embedded systems, sensor networks, radio networks, short range inductive links, and capacitive sensing techniques.

JUSSI T. KOIVUMÄKI received the Ph.D. degree in biophysics from the University of Oulu, Finland, in 2009. He is currently an Adjunct Professor (Docent) in computational cardiac cell electromechanics with the Computational Biophysics and Imaging Group, Faculty of Medicine and Health Technology, and an Adjunct Professor (Docent) in computational physiology with the University of Eastern Finland. His research interests include mathematical modeling, computational physiology, cardiac physiology, arrhythmias, heart failure, cardiac development, teaching, confocal microscopy, biotechnology, and biomedicine.

HEIMO IHALAINEN started teaching measurement technology at the Tampere University of Technology, in 1974, and is doing research at multivariate signals in the 1990s. At the beginning of the 2000s, he started working on a new topic, measurement based on images, and though he is officially retired now, the topic motivates him to continue working in the field.

KATRIINA AALTO-SETÄLÄ received the M.D. degree. She is currently a Professor of physiology with the Faculty of Medicine and Life Sciences, University of Tampere, and a Cardiologist with the Heart Hospital, Tampere University Hospital, Finland. She currently works as an Invasive Cardiologist and is in charge of the genetic cardiac outpatient clinic at the Heart Hospital. Her research at the University of Tampere focuses on human genetic cardiac diseases, such as genetic arrhythmias and atherosclerosis with the help of induced pluripotent stem cell (iPSC) technology. The main aim of the research group is to learn more about the basic pathology of the genetic diseases as well as to test current and new pharmaceutical agents to correct the abnormalities. Her research group in collaboration with researchers at the Tampere University of Technology has also invented new methods to monitor and analyze the maturity and functionality of cardiomyocytes.

PASI KALLIO received the M.S. degree in electrical engineering and the D.Tech. degree in automation engineering from the Tampere University of Technology (TUT), Tampere, Finland, in 1994 and 2002, respectively. Since 2008, he has been a Professor of automation engineering with TUT, where he is currently the Vice Director of the Faculty of Biomedical Sciences and Engineering. He has authored more than 130 articles, and has more than ten patent applications. His current research interests include microrobotics, microfluidics, and their automation in cell and tissue engineering, medical diagnostics, and soft material testing applications. He was the Chair of the IEEE Finland Section, from 2012 to 2013. He was a recipient of the Finnish Automation Society Award, in 2009.

JUKKA LEKKALA received the M.Sc. degree in electronics and the D.Sc. (Tech.) degree in biomedical engineering from the Tampere University of Technology (TUT), Tampere, Finland, in 1979 and 1984, respectively. From 1985 to 2001, he has worked as a Senior Research Scientist with VTT (Technical Research Centre of Finland) in different research units developing biosensor technology and sensor materials. In 1991, he was appointed as a Docent of bioelectronics at the University of Oulu, and a Docent of biomedical engineering at TUT. Since 2002, he has been a Professor of automation engineering at TUT. He is currently a Professor Emeritus with the Faculty of Biomedical Sciences and Engineering (TUT-BMT). He has more than 170 scientific publications and ten patents. His research interests include sensors, measurement systems, and biosensing.